

Structural analysis of metalorganic chemical vapor deposited AlN nucleation layers on Si (111)

Zang Keyan¹, Wang Lianshan², Chua Soo Jin^{1,2}, Carl V. Thompson^{1,3}

¹ Singapore-MIT Alliance, E4-04-10, NUS, 4 Engineering Drive 3, Singapore 117576

² Institute of Materials Research & Engineering, 3 Research Link, 117602, Singapore

³ Department of Materials Science and Engineering, MIT, Cambridge, Massachusetts 02139

Abstract—AlN nucleation layers are being investigated for growth of GaN on Si. The microstructures of high-temperature AlN nucleation layers grown by MOCVD on Si (111) substrates with trimethylaluminum pre-treatments have been studied using atomic force microscopy (AFM) and transmission electron microscopy (TEM). The AFM results show that with TMA pre-treatments, AlN grows in a pseudo-2-dimensional mode because the lateral growth rate of AlN is increased, and the wetting property of the AlN on silicon is improved. Also, no amorphous SiN_x layer was observed at the interface with TMA pre-treatments and AlN films with good epitaxial crystalline quality were obtained. Transmission electron diffraction patterns revealed that the AlN and Si have the crystallographic orientation relationship $\text{AlN} [0001] \parallel \text{Si} [111]$ and $\text{AlN} [11\bar{2}0] \parallel \text{Si} [110]$. High resolution transmission electron microscopy indicates a 5:4 lattice matching relationship for AlN and Si along the Si [110] direction. Based on this observation, a lattice matching model is proposed.

Index Terms— Metal-organic Chemical Vapour Deposition, III-V Nitrides

I. INTRODUCTION

GaN-on-silicon offers very attractive potential for the manufacturability and cost benefits for GaN optoelectronic and microelectronic devices. The growth of high quality of GaN on silicon has been reported earlier [1-3], and devices such as LED's and UV detectors have been fabricated [2, 4]. For the growth of crack-free, device-quality GaN-on-silicon, both the large lattice mismatch and positive thermal expansion coefficient difference must be overcome. The strong reaction between Si and Ga during the growth of LT-GaN results in poor crystal quality and morphology of the GaN film [5]. Also, there is a strong tendency towards the formation of amorphous SiN_x, which will induce 3-dimensional growth and polycrystalline GaN. GaN is therefore not well suited for *direct* epitaxial growth on silicon substrates. Use of AlN as an intermediate buffer layer is one of the most promising ways to achieve high quality of GaN on Si, and this approach has been widely studied in MOCVD and MBE system [6-10]. Compared to Si, AlN has smaller lattice mismatch (2.4% vs. 19%) and difference in thermal expansion coefficient (+26% vs 100%) with GaN. Even though there still exists 23.4% lattice misfit between AlN and Si, wurtzite AlN can be grown on Si (111) with good

structural properties and smooth surface morphology [11-13]. The reason is due to a lattice coincidence between Si (111) and wurtzite AlN for certain crystallographic orientations, and the relaxation of the stress via a large number of misfit dislocation at the Si/AlN interface [14].

It is observed that an amorphous SiN_x layer can form at the AlN-silicon interface, which would degrade the quality of AlN and GaN films [15-18]. To prevent the formation of such amorphous layers, Al has been deposited on the silicon surface before the deposition of AlN, both in MOCVD and MBE systems [19-21]. Using such an Al pre-treatment, high quality of GaN was achieved on silicon in a GS-MBE system by Nikishin [19, 20]. While two dimensional growth of AlN has been achieved in MBE systems, this growth mode for AlN buffers has not been observed in MOCVD. Since the buffer layer serves as the crystallographic and morphological template for subsequent GaN deposition, the microstructure and growth mode of this layer must be understood to achieve device-quality GaN on silicon substrates.

In this paper, we report on the effect of TMA pretreatments on the microstructure of AlN nucleation layers in MOCVD growth, and we also report on the growth of single crystalline wurtzite AlN films with different thickness. The films were characterized using Atomic Force Microscopy (AFM), and Transmission Electron Microscopy (TEM). The interface of AlN and Si substrates has been studied combining the use of TEM images and atomic ball-and-stick models of the interface.

II. EXPERIMENTAL DETAILS

Boron-doped Si (111) wafers with resistivities of 1-4 Ω·cm were used as substrates. The substrates were cleaned using the RCA recipe followed by dipping into an HF solution to form a hydrogen-terminated surfaces. The growth was carried out in an EMCORE-D125 MOCVD system. Hydrogen was used as the carrier gas. Trimethylaluminum (TMA), and ammonia (NH₃) were used as the precursors for Al and N, respectively. Before growing AlN, the substrate was baked in an H₂ ambient at 1000°C for 15min to remove the native oxide. TMA was introduced for 6 seconds before the introduction of ammonia into the chamber at 1010°C. The AlN layer was then initially grown by introducing ammonia into the growth chamber and was

grown for 10min, 30min, and 60minutes. The flow rates of TMA and NH_3 for AlN growth were $200\mu\text{mol}/\text{min}$ and $0.45\text{mol}/\text{min}$. The reactor pressure was 50Torr. The AlN layer was characterized using atomic force microscopy (AFM) in tapping mode and transmitted electrical microscopy (TEM).

III. RESULTS AND DISCUSSION

We reported the micro-structural evolution of AlN nucleation layer without TMA pre-treatment in a previous paper [18]. The microstructure of an AlN layer grown for 10 minutes exhibited 3 dimensional nuclei formed on the silicon surface with a density of $2.2 \times 10^{11} / \text{cm}^2$. With the growth time extended to 80 minutes, the AlN nuclei covered the whole surface of Si with an average island size of 120nm, poor single crystalline AlN with mis-oriented domains and stacking faults was formed. Also, an amorphous SiN_x at the interface of AlN layer and Si was observed using cross-sectional TEM.

To prevent formation of an amorphous layer at the interface, TMA was flowed for a few seconds before the reaction of TMA and ammonia at high temperature. The surface morphology and crystalline structure of AlN layers were studied using AFM and TEM.

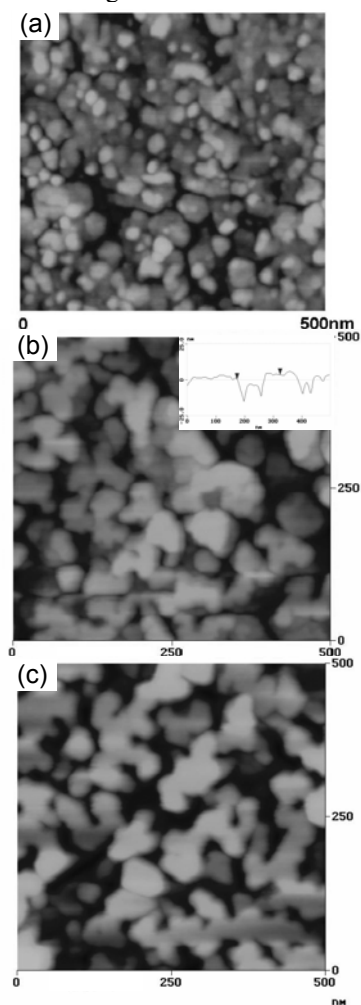
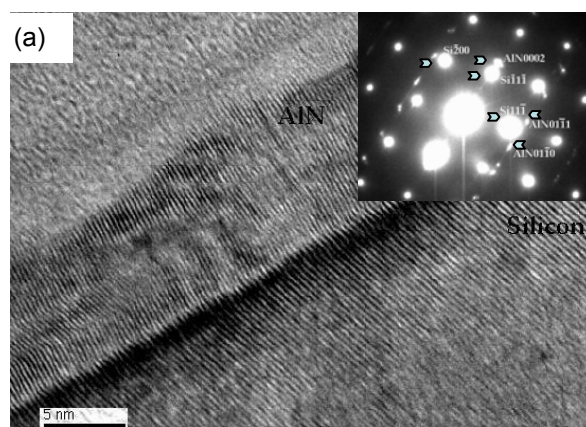


FIG. 1. Tapping mode AFM images of AlN buffer layers: (a) as-grown layer with growth time of 10min, (b) as-grown layer with growth time of 30min, (c) as-grown layer with growth time of 60min. All these samples were deposited with TMA pre-treatment of the silicon surface before the growth of AlN. The scan area is 500nm.

The initial stages of AlN nucleation on silicon were first examined using tapping mode AFM. Fig.1 shows AFM micro-graphs of as-grown nucleation layers after 10-min growth (Fig. 1a: 7 nm nominal thickness as evidenced in TEM images), 30-min growth (Fig. 1b: 15nm nominal thickness), and 60-min growth (Fig. 1c: 20nm nominal thickness). From Fig. 1a, we observed that with TMA pre-treatments, the grain size can extend to larger than 40nm while the height of the grain is only 5-8nm at the initial stage of growth (Fig. 1a). TMA pre-treatment increase the wetting of AlN on silicon and the surface mobility of Al and nitrogen is increased as indicated by the increased lateral growth rate of AlN to form a wetting layer of AlN on the silicon surface. Based on the AFM image (Fig. 1a); we proposed that 3-dimensional AlN nuclei were formed on silicon substrate at the very initial growth stage (extending from several seconds to several minutes) [18]. These nuclei grew with very high lateral growth rates compared to vertical growth rates, due to the wetting properties of AlN after TMA pre-treatments. This lateral growth leads to coalescence to form AlN films with sub-grains. Above the coalesced AlN layer, more AlN nuclei were formed with continued deposition. With longer growth times (as seen from Fig. 2b and 2c), the grains underwent lateral and vertical growth with higher overall lateral growth rates, and coalesced laterally. As a result, two-dimensional islands with sizes larger than 200nm were observed in the resulting images. Those islands have relatively flat surfaces (Fig.1b insertion) as a result of their lateral growth. This high lateral growth rate results in a pseudo-2-dimensional growth mode of the AlN. The growth parameters could be optimized to increase the lateral growth rate of the AlN layers and to lead to layer-by-layer growth.



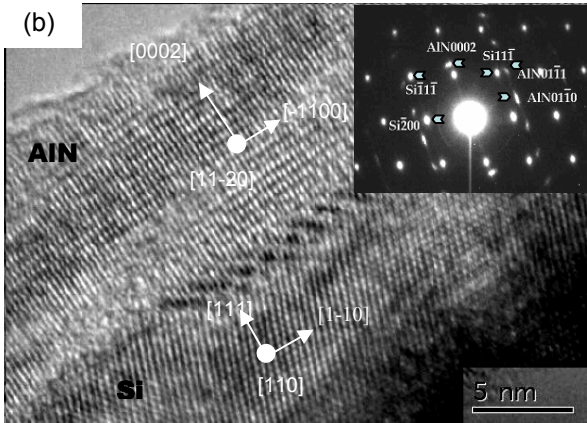


FIG. 2. Cross-sectional HRTEM image of AlN epilayers (a) grown for 10 minutes and (b) grown for 60 minutes on Si (111) substrates with TMA pre-treatments. AlN buffer layers showed the hexagonal single crystalline structure with high epitaxial crystalline quality. An amorphous layer of SiN_x can not be observed at the interface of the AlN and Silicon. Insertions are the selected area diffraction patterns of the interfacial region between AlN and the silicon substrate, with the electron beam parallel to the [110]Si direction.

In Fig. 2, the results of cross-sectional high resolution TEM studies of the as-grown AlN nucleation layer for 10min (Fig. 2a) and 60min (Fig. 2b) are presented. From the images, we observe that single crystalline AlN layers have grown epitaxially on Si (111) when TMA pretreatments were used. The corresponding diffraction patterns shows the crystallographic orientation of Si and AlN has the relationship $[11\bar{2}0] \text{ AlN} \parallel [110] \text{ Silicon}$ and $[0002] \text{ AlN} \parallel [111] \text{ Silicon}$. Other relationships have also been reported for MBE growth, with $\text{AlN} [2\bar{1}\bar{1}0] \parallel \text{Si} [0\bar{2}\bar{2}]$ and $\text{AlN} [10\bar{1}0] \parallel \text{Si} [02\bar{2}]$ co-existing in the film[7]. In addition, in MBE-grown films, an average misalignment along the c-axis of 1.8° and 3° was also estimated using a coordinate transformation of the electron diffraction pattern [9].

With TMA pretreatment of the silicon surface, the interface between AlN and silicon tends to be sharp and no amorphous layer can be observed at the interface (Fig. 2). Formation of an amorphous layer was suppressed, and the AlN film provided a better template for the subsequent growth of GaN.

With the observed crystallographic relationship between AlN and silicon, a large lattice mismatch (19%) exists between the epilayers and the substrates. To relax such large mismatch strain, a periodic array of misfit dislocation was formed at the first monolayer of the interface as observed in high resolution TEM images (figure 3c). The diagram in figure 3a illustrates a projection of the bulk basal plane for (111) silicon and the AlN cation positions for the epitaxial orientation observe in our experiments. Along the AlN $[\bar{1}100]$ direction, there is a periodic coincident of atoms at the interface (arrows in

figure 3a). Between these coincident sites along the AlN $[\bar{1}100]$ direction, viewed from AlN $[11\bar{2}0]$ direction, one misfit dislocation introduced on the AlN side of the interface can achieve a near-coincidence of 5 AlN lattice spacings to 4 silicon lattice spacings. Even though a large density of misfit dislocations forms, there is still a 1.3% mismatch between the epilayers and silicon substrates [19], because other atoms are not completely coincident with each other. Fig. 2b shows a ball-and-stick-model of the atomic arrangement at the AlN and silicon interface, viewed along AlN $[11\bar{2}0]$ and Si $[110]$ directions. Corresponding to Fig. 3a, one misfit dislocation was formed between to coincident atoms to partially relax the strain.

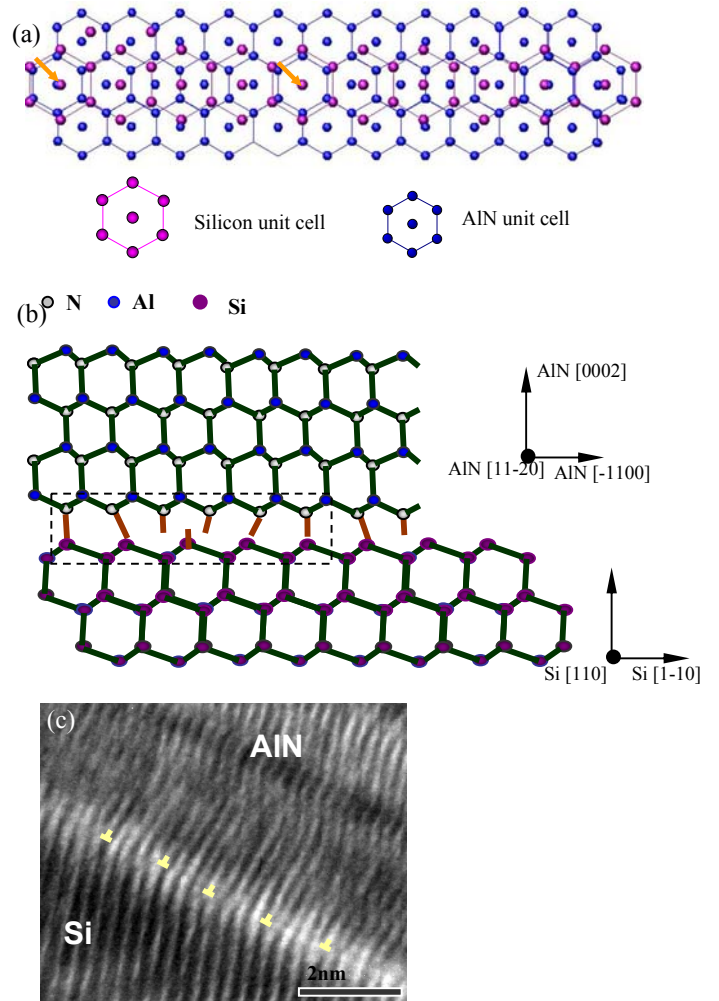


FIG. 3. (a) Projection of the bulk basal plane of (111) silicon and the AlN cation positions for the observed epitaxial growth orientation. Arrows indicate the coincidence of the AlN atoms with silicon (111) atoms. The figure was drawn with the actual ratio of AlN and silicon lattice parameters. (b) A ball-and-stick-model of the atomic arrangement of AlN and silicon, viewed along the AlN $[11\bar{2}0]$ and Si $[110]$ directions. Corresponding to Fig. 3a, misfit dislocations were introduced to relax the the misfit strain between coincidence sites. (c) Cross-sectional

high resolution TEM at the interface AlN grown for 30min Si. Misfit dislocations are indicated in the images.

IV CONCLUSION

Good quality epitaxial AlN films were grown on silicon (111) using MOCVD. Pretreatments with TMA helps prevent formation of amorphous SiN_x layers and promotes wetting of AlN on the Si so that a pseudo-two-dimensional growth mode lead to formation of the AlN layer. Formation of SiN_x would otherwise occur due to the reaction of the Si substrate with ammonia at the initial stages of growth. Semi-coherent interfaces can be formed at the AlN-silicon interface with the relationship AlN [0002] || Si[111] and AlN[11 2 0] || Si[110]. An array of misfit dislocations was formed in the first AlN to reduce the strain due to lattice mismatch.

REFERENCES

- [1] T. Takeuchi, H. Amano, K. Hiramatsu, N. Sawaki, and I. Akasaki, *J. Cryst. Growth* 115, 634 (1991)
- [2] S. Guha and N. A. Bojarczuk, *Appl. Phys. Lett.* 72, 415 (1998)
- [3] F. Semond, B. Damilano, S. Vezian, N. Granjean, M. Leroux, and J. Massies, *Appl. Phys. Lett.* 75, 82 (1999)
- [4] A. Osinsky, S. Gangopadhyay, J. W. Yang, R. Gaska, D. Kuksenkov, H. Temkin, I. K. Shmagin, Y. C. Chang, J. F. Muth, R.M. Kolbas, *Appl. Phys. Lett.* 72, 551 (1998)
- [5] Alois Krost, Armin Dadgar, *Materials Science and Engineering*, B93, 77 (2002)
- [6] A. Watanabe, T. Takeuchi, K. Hirosawa, H. Amano, K. Hiramatsu and I. Akasaki, *J. Cryst. Growth*, 128, 391 (1993)
- [7] A. Bourret, A. Barski, J. L. Rouviere, G. Renaud, and A. Barbier, *J. Appl. Phys.*, 83, 2003 (1998)
- [8] Eric Rehder, M. Zhou, L. Zhang, N. R. Perkins, S. E. Babcock, and T. F. Kuech, *MRS Internet J. Nitride Semicond. Res.* 4S1, G3.56 (1999)
- [9] H.M. Liaw, R. Doyle, P.L. Fejes, S. Zollner, A. Konkar, K.J. Linthicum, T. Gehrke, R.F. Davis, *Solid-state Electronics*, 44, 747 (2000)
- [10] S. Kaiser, M. Jakob, J. Zweck, and W. Gebhardt, et al, *J. Vac. Sci. Technol. B* 18(2): 733 (2000)
- [11] V. Lebedev, B. Schröter, G. Kipshidze, Wo. Richter, *J. Crystal Growth* 207 (1999) 266
- [12] A.T. Schremer, J.A. Smart, Y. Wang, O. Ambacher, N.C. MacDonald, J.R. Shealy, *Appl. Phys. Lett.* 76, 736 (2000)
- [13] S.I. Molina, A.M. Sanchez, F.J. Pacheco, R. Garcia, M.A. Sanchez-Garcia, F.J. Sanchez, E. Calleja, *Appl. Phys. Lett.* 74 (1999) 3362
- [14] H.P.D. Schenk, U. Kaiser, G.D. Kipshidze, A. Fissel, J. Kraußlich, H. Hobert, J. Schulze, Wo. Richter, *Materials Science and Engineering*, B59 (1999) 84–87
- [15] G. Q. Hu, X. Kong, L. Wang, Y. Q. Wang, X. F. Duan, Y. Lu, X. L. Liu, *J. of Crystal Growth*, 256 (2003), 416
- [16] Min-Ho, Young-Churl Bang, Nae-Man Park, Chel-Jong Choi, Tae-Yeon Seong, and Seong-Ju Park, *Appl. Phys. Lett.*, 78 (2001) 2858
- [17] Shigeyasu Tanaka, Yasutoshi Kawaguchi, and Nobuhiko Sawaki, et al, *Applied Physics Letters*, 76, (2000) 2701
- [18] K. Y. Zang, S. J. Chua, L. S. Wang and C. V. Thompson, *phys. Stat. sol.* In press
- [19] S. A. Nikishin, V. G. Antipov, S. Francoeur, N. N. Faleev, G. A. Seryogin, V. A. Elyukhin, and H. Temkin, et al, *Applied Physics Letters*, 75, (1999) 484
- [20] S. A. Nikishin, N. N. Faleev, V. G. antipov, S. Francoeur, L. Grave de Paralta, G. A. Seryogin, and H. Temkin, et al, *Appl. Phys. Lett.* 75, (1999) 2073
- [21] P. Chen, R. Zhang, Z. M. Zhao, D. J. Xi, B. Shen, Z.Z. Chen, Y.G. Zhou, S.Y. Xie, W.F. Lu, Y.D. Zheng, *Journal of Crystal Growth*, 225, (2001) 150